

Alleviating the $\bar{B} \rightarrow D\tau\nu_\tau$ and $\bar{B} \rightarrow D^*\tau\nu_\tau$ puzzle in the MSSM

Dris Boubaa^{1,2,3}, Shaaban Khalil³ and Stefano Moretti¹

¹ *School of Physics and Astronomy, University of Southampton, Highfield, Southampton SO17 1BJ, UK*

² *Département de Physique, Faculté des Sciences Exactes et Informatique, Université Hassiba Benbouali de Chlef, Pôle Universitaire d'Ouled Fares, 02180, Chlef, Algérie*

³ *Center for Fundamental Physics, Zewail City of Science and Technology, Sheikh Zayed, 12588, Giza, Egypt*

E-mail: d.boubaa@soton.ac.uk
skhalil@zewailcity.edu.eg
s.moretti@soton.ac.uk

Abstract

We show that Supersymmetric effects driven by penguin contributions to the $b \rightarrow c\tau\nu_\tau$ transition are able to account simultaneously for a sizeable increase of both branching ratios of $\bar{B} \rightarrow D\tau\bar{\nu}_\tau$ and $\bar{B} \rightarrow D^*\tau\bar{\nu}_\tau$ with respect to the Standard Model predictions, thereby approaching their experimentally measured values. We emphasise that a light chargino and neutralino, with masses less than 300 GeV, in addition to a large stau/sneutrino mass and a large $\tan\beta$, are essential for enhancing the effect of the lepton penguin $\tau\nu_\tau W^\pm$, which is responsible for the improved theoretical predictions with respect to current data.

1 Introduction

Rare B -decays provide a good opportunity for probing New Physics (NP) Beyond the Standard Model (BSM). In fact, experimental studies of flavour at (Super) B -factories (BaBar and Belle) and LHCb are complementary to the direct search for NP at the Large Hadron Collider (LHC). The origin of flavour and Charge-Parity (CP) violation is one of the most profound open questions in particle physics. Most extensions of the SM, wherein the latter is embedded as a low energy effective theory, include new sources of flavour and CP violation. Supersymmetry (SUSY) is one promising candidate for BSM physics which has these characteristics, particularly if the soft SUSY-breaking terms are non-universal.

It has been recently reported a deviation from the SM expectations in the ratios

$$R(D) = \frac{\text{BR}(\bar{B} \rightarrow D\tau\bar{\nu}_\tau)}{\text{BR}(\bar{B} \rightarrow D\ell\bar{\nu}_\ell)}, \quad R(D^*) = \frac{\text{BR}(\bar{B} \rightarrow D^*\tau\bar{\nu}_\tau)}{\text{BR}(\bar{B} \rightarrow D^*\ell\bar{\nu}_\ell)}, \quad (1)$$

where ℓ refers to either electron or muon. On the one hand, between 2015 and 2017, the Belle collaboration [1, 2, 3, 4] has reported the following results:

$$R(D)^{\text{Belle}} = 0.375 \pm 0.064, \quad (2)$$

$$R(D^*)_{\text{ave}}^{\text{Belle}} = 0.288 \pm 0.019. \quad (3)$$

On the other hand, the BaBar collaboration found that [5]

$$R(D)^{\text{BaBar}} = 0.440 \pm 0.072, \quad (4)$$

$$R(D^*)^{\text{BaBar}} = 0.332 \pm 0.030. \quad (5)$$

In addition, the LHCb collaboration has announced the following value for $R(D^*)$ [6]:

$$R(D^*)^{\text{LHCb}} = 0.336 \pm 0.027 \pm 0.030. \quad (6)$$

Therefore, the overall combined average is given by [7]:

$$R(D) = 0.403 \pm 0.040, \quad (7)$$

$$R(D^*) = 0.310 \pm 0.015, \quad (8)$$

which deviate by $\sim 1.7\sigma$ for $R(D)$ and $\sim 3.9\sigma$ for $R(D^*)$ from the SM expectations that are given by [8, 9, 10]

$$R(D)^{\text{SM}} = 0.305 \pm 0.012, \quad (9)$$

$$R(D^*)^{\text{SM}} = 0.252 \pm 0.004. \quad (10)$$

These deviations, if confirmed, could be important hints for NP, especially because the SM results for $R(D)$ and $R(D^*)$ are essentially independent of the parameterisation of the hadronic matrix elements.

As the semileptonic decay $b \rightarrow c\tau\nu_\tau$ takes place in the SM at tree level, it is naively expected that any BSM contribution would be subdominant, even those embedding a charged Higgs boson entering at tree-level, since $M_{H^\pm} \geq M_{W^\pm}$. Indeed, it is notoriously challenging to account for large deviations from the SM rates. This has been shown explicitly in some SM extensions [11, 12, 13, 14, 15]. In particular, it was emphasised that in 2-Higgs Doublet Models (2HDMs) the above experimental results for $R(D)$ and $R(D^*)$ cannot be simultaneously explained.

In this article we argue that SUSY contributions, as described in the Minimal Supersymmetric Standard Model (MSSM) with non-universal soft SUSY-breaking terms, might help to explain the discrepancy between the experimental results for $\bar{B} \rightarrow D\tau\nu_\tau$ and $\bar{B} \rightarrow D^*\tau\nu_\tau$ and the corresponding SM expectations. For the first time in literature, to our knowledge, we consider here all contributions up to Next-to-Leading Order (NLO) within the MSSM: tree-level ones due to charged gauge boson and Higgs exchange as well as one-loop ones due to bubbles, triangles (penguins) and boxes onset by the exchanges of 2HDM states (i.e., γ , Z , W^\pm , H^\pm , h^0 , H^0 and A^0) alongside the SUSY ones due to gauginos (charginos and neutralinos) and sfermions (squarks, sleptons and sneutrinos). Our results ameliorate the situation with respect to the aforementioned data, yet even higher orders may be required to achieve full consistency.

The plan of the paper is as follows. In the next section we describe the calculation in some detail in terms of helicity amplitudes and corresponding observables. In Sect. 3 we introduce the Wilson coefficients needed for the calculation. Then we describe the experimental constraints enforced and illustrate our numerical analysis. We finally conclude in Sect. 6.

2 Model Independent Contributions to $R(D)$ and $R(D^*)$

The effective Hamiltonian for $b \rightarrow c\bar{l}\nu_l$ is given by

$$\begin{aligned} \mathcal{H}_{\text{eff}} = & \frac{4G_F V_{cb}}{\sqrt{2}} \left[(1 + g_{VL}) [\bar{c}\gamma_\mu P_L b] [\bar{l}\gamma_\mu P_L \nu_l] + g_{VR} [\bar{c}\gamma_\mu P_R b] [\bar{l}\gamma_\mu P_L \nu_l] \right. \\ & \left. + g_{SL} [\bar{c}P_L b] [\bar{l}P_L \nu_l] + g_{SR} [\bar{c}P_R b] [\bar{l}P_L \nu_l] + g_T [\bar{c}\sigma^{\mu\nu} P_L b] [\bar{l}\sigma_{\mu\nu} P_L \nu_l] \right], \end{aligned} \quad (11)$$

where G_F is the Fermi coupling constant, V_{cb} is the Cabibbo-Kobayashi-Maskawa (CKM) matrix element between charm and bottom quarks while $P_{L/R} = (1 - / + \gamma_5)/2$. Further, g_i is defined in terms of the Wilson coefficients (see [16] for prospects of extracting these using optimal observables) C_i as

$$g_i = \frac{C_i^{\text{SUSY}}}{C_i^{\text{SM}}}, \quad i \equiv VL, VR, SL, SR, T \quad (12)$$

with $C^{\text{SM}} = \frac{4G_F V_{cb}}{\sqrt{2}}$. Therefore, the full amplitude $\bar{B} \rightarrow D l \bar{\nu}_l$ takes the form

$$\mathcal{M} = \mathcal{M}_{\text{SM}}^{\lambda_{D^{(*)}}, \lambda_l} + \mathcal{M}_{S(L,R)}^{\lambda_{D^{(*)}}, \lambda_l} + \mathcal{M}_{V(L,R)}^{\lambda_{D^{(*)}}, \lambda_l} + \mathcal{M}_T^{\lambda_{D^{(*)}}, \lambda_l}, \quad (13)$$

where λ_l is the helicity of the lepton l . The $D^{(*)}$ -meson is taken to be either a spin-0 D -meson, with $\lambda_D = 0$, or a spin-1 D^* -meson, with $\lambda_{D^*} = \pm, 0$.

Furthermore, one can define both observables $R(D)$ and $R(D^*)$ as follows:

$$R(D) = \frac{\Gamma(\bar{B} \rightarrow D \tau \nu_\tau)}{\Gamma(\bar{B} \rightarrow D l \nu_l)}, \quad R(D^*) = \frac{\Gamma(\bar{B} \rightarrow D^* \tau \nu_\tau)}{\Gamma(\bar{B} \rightarrow D^* l \nu_l)}. \quad (14)$$

Using the explicit formulae of the hadronic and leptonic amplitudes in Refs. [8, 9, 17, 18, 19, 20] (when the l

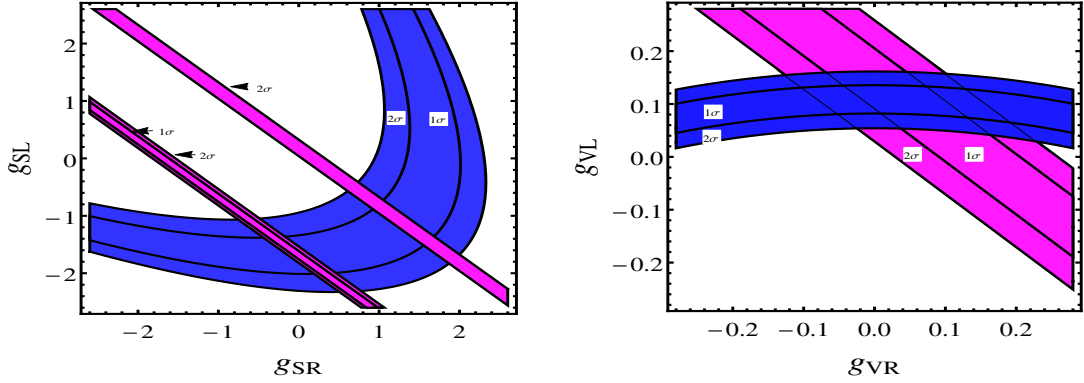


Figure 1: The allowed regions in the (g_{SL}, g_{SR}) (left) and (g_{VL}, g_{VR}) (right) planes by the 1σ and 2σ experimental results on $R(D)$ (magenta) and $R(D^*)$ (blue) of the combined average.

contribution is assumed to be described by the SM¹⁾ and upon fixing the SM parameters as well as the form factors involved in the definition of the matrix elements to their central values as in Ref. [5], we can cast the explicit dependence of $R(D)$ and $R(D^*)$ upon the Wilson coefficients in the MSSM as follows:

$$R(D) = R(D)^{\text{SM}} \left[0.981 |g_{SR} + g_{SL}|^2 + |1 + g_{VL} + g_{VR}|^2 + 0.811 |g_T|^2 + 1.465 \text{Re}[(1 + g_{VL} + g_{VR}) \times (g_{SR} + g_{SL})^*] + 1.074 \text{Re}[(1 + g_{VL} + g_{VR}) g_T^*] \right], \quad (15)$$

$$R(D^*) = R(D^*)^{\text{SM}} \left[0.025 |g_{SR} - g_{SL}|^2 + |1 + g_{VL}|^2 + |g_{VR}|^2 + 16.739 |g_T|^2 + 0.094 \text{Re}[(1 + g_{VL} + g_{VR}) \times (g_{SR} - g_{SL})^*] + 6.513 \text{Re}[g_{VR} g_T^*] - 4.457 \text{Re}[(1 + g_{VL}) g_T^*] - 1.748 \text{Re}[(1 + g_{VL}) g_{VR}^*] \right]. \quad (16)$$

Thus, in case of a dominant scalar contribution (and negligible vector and tensor ones), it is clear that $R(D^*)$ cannot be significantly larger than the SM expectation, due to the smallness of the coefficient of this contribution,

¹This assumption is made here only for convenience, so as to write model independent analytical formulae. In the next sections though, SUSY contributions are analysed for all processes: $\bar{B} \rightarrow D \tau \nu_\tau$ and $\bar{B} \rightarrow D l \nu_l$, i.e.,

$$R(D) = \frac{\text{BR}(B \rightarrow D \tau \nu)^{\text{SM+SUSY}}}{\text{BR}(B \rightarrow D l \nu)^{\text{SM+SUSY}}}.$$

In presence of experimental constraints on $\text{BR}(\bar{B} \rightarrow D l \nu_l)$, which are in fact quite consistent with the SM results, i.e., $\text{BR}(B \rightarrow D l \nu)^{\text{SM+SUSY}}$ is within the experimental range of the measured $\text{BR}(B \rightarrow D l \nu)$ (similar arguments hold for the B^* rates).

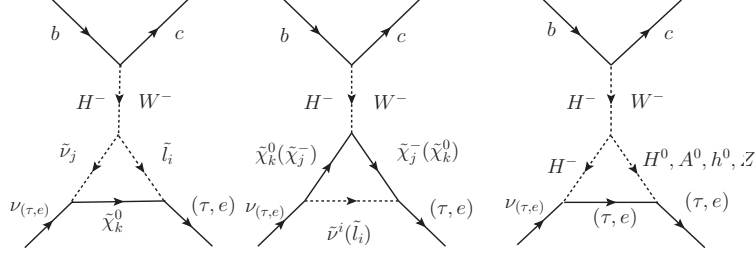


Figure 2: Triangle diagrams (penguins) contributing to, e.g., $b \rightarrow c(\tau, e)\nu_{(\tau, e)}$ affecting the leptonic vertex.

unless $|g_{SR} - g_{SL}|$ is much larger than 1 (i.e., $C_S^{\text{SUSY}} > C^{\text{SM}}$), which is not possible. Recall that g_{SR} is larger than g_{SL} and receives a contribution at the tree-level via charged Higgs boson (H^\pm) exchange that yields

$$g_{SR} = \frac{-m_b m_\tau \tan \beta^2}{M_{H^\pm}^2}. \quad (17)$$

This conclusion is confirmed in Fig. 1, where we display the regions in the (g_{SL}, g_{SR}) plane that can accommodate the experimental results of $R(D)$ and $R(D^*)$ within 1σ and 2σ Confidence Level (CL) for, e.g., Belle, the experiment with predictions closer to the SM. From this figure, it is clear that the scalar contribution alone cannot account for both $R(D)$ and $R(D^*)$ simultaneously. In order to get $R(D)$ and $R(D^*)$ within 2σ of the aforementioned average results from the various experiments, (g_{SL}, g_{SR}) should lie between $[-2.32, -0.77]$ and $[-0.39, 2.03]$, respectively. In these conditions, either g_{SL} or g_{SR} is larger than 1, which is not possible.

In case of a dominant vector contribution, as shown from the allowed regions of (g_{VL}, g_{VR}) in Fig. 1, one gets $R(D)$ and $R(D^*)$ inside the 2σ region of the averages if (g_{VL}, g_{VR}) varies between $(0.05, 0.02)$ and $(0.15, 0.10)$, respectively. Furthermore, it is remarkable that, unlike the scalar contribution, a small vector contribution, $g_{VL} \sim \mathcal{O}(0.1)$ and $g_{VR} \sim \mathcal{O}(0.01)$, can induce significant enhancement for both $R(D)$ and $R(D^*)$: e.g., $R(D) \sim 0.336$ and $R(D^*) \sim 0.277$ if $g_{VL} \sim 0.05$ and $g_{VR} \sim 0$, which, as we will see, are quite plausible values in the MSSM. Finally, the tensor contribution, which is typically quite small, may affect only $R(D^*)$.

3 SUSY Contributions to $b \rightarrow c\tau\nu_\tau$

The SUSY contributions to g_{VL} are generated from the penguin corrections to the vertex $W^\pm l\nu_l$ ($l = e, \mu, \tau$) through the exchange of charginos and neutralinos alongside sleptons and sneutrinos, respectively, as displayed in Fig. 2. Our calculation is based on FlavorKit [21], SARAH [22] and SPheno [23], although the dominant penguin corrections were also derived analytically. Renormalisation is performed at one loop using the $\overline{\text{DR}}$ scheme (following SARAH and SPheno) including the full momentum dependence for any SUSY and Higgs state. As a cross-check of the implementation, we have explicitly verified that, while our loop integrals for the two and three point functions depend upon the renormalisation scale, such a dependence drops out in the computation of physical observables. In fact, it can be extracted from our equations that the loop corrections scale with v^2/M_{SUSY}^2 , so that, in the limit of very large M_{SUSY} , the loop effects go to zero, hence $R(D)$ and $R(D^*)$ approach their SM values. In order to have sizable loop functions, we will enforce on our scans the condition $m_{\tilde{\chi}_1^0} \approx m_{\tilde{\chi}_1^\pm} \lesssim 500$ GeV.

Let us now try to decode our results, by concentrating on the Wilson coefficient C_{VL} , which sees contributions induced by the penguin topologies in Fig. 2. Firstly, we can confirm that the graph with neutral Higgs bosons is small while the other two are roughly comparable. Thus, the emerging C_{VL}^{SUSY} term is essentially

$$C_{VL}^{\text{SUSY}} = C_{VL}^{\tilde{\tau}} + C_{VL}^{\tilde{\nu}} + C_{VL}^{(A^0, H^0, h^0)}, \quad (18)$$

where

$$C_{VL}^{\tilde{\tau}} = \frac{\Gamma_{\tilde{\chi}_j^- \nu_{l_I} \tilde{\tau}_i^*}^L \Gamma_{\tilde{l}_I \tilde{\chi}_k^0 \tilde{\tau}_i}^R \Gamma_{\tilde{c} b W^-}^L}{16\pi^2 M_{W^\pm}^2} \left[\Gamma_{\tilde{\chi}_j^+ \tilde{\chi}_k^0 W^-}^R m_{\tilde{\chi}_j^-} m_{\tilde{\chi}_k^0} C_0(m_{\tilde{\chi}_k^0}^2, m_{\tilde{\chi}_j^-}^2, m_{\tilde{\tau}_i}^2) \right. \\ \left. - \Gamma_{\tilde{\chi}_j^+ \tilde{\chi}_k^0 W^-}^L (B_0(m_{\tilde{\chi}_j^-}^2, m_{\tilde{\chi}_k^0}^2) - 2C_{00}(m_{\tilde{\chi}_k^0}^2, m_{\tilde{\chi}_j^-}^2, m_{\tilde{\tau}_i}^2) + m_{\tilde{\tau}_i}^2 C_0(m_{\tilde{\chi}_k^0}^2, m_{\tilde{\chi}_j^-}^2, m_{\tilde{\tau}_i}^2)) \right], \quad (19)$$

$$C_{VL}^{\tilde{\nu}} = \frac{\Gamma_{\nu_{l_I} \tilde{\chi}_k^0 \tilde{\nu}_i^*}^L \Gamma_{\tilde{\chi}_j^- \tilde{l}_I \tilde{\nu}_i}^R \Gamma_{\tilde{c} b W^-}^L}{16\pi^2 M_{W^\pm}^2} \left[-\Gamma_{\tilde{\chi}_j^+ \tilde{\chi}_k^0 W^-}^L m_{\tilde{\chi}_j^-} m_{\tilde{\chi}_k^0} C_0(m_{\tilde{\chi}_j^-}^2, m_{\tilde{\chi}_k^0}^2, m_{\tilde{\nu}_i}^2) \right. \\ \left. + \Gamma_{\tilde{\chi}_j^+ \tilde{\chi}_k^0 W^-}^R (B_0(m_{\tilde{\chi}_k^0}^2, m_{\tilde{\chi}_j^-}^2) - 2C_{00}(m_{\tilde{\chi}_j^-}^2, m_{\tilde{\chi}_k^0}^2, m_{\tilde{\nu}_i}^2) + m_{\tilde{\tau}_i}^2 C_0(m_{\tilde{\chi}_j^-}^2, m_{\tilde{\chi}_k^0}^2, m_{\tilde{\nu}_i}^2)) \right], \quad (20)$$

$$C_{VL}^{A^0} = \frac{2\Gamma_{\tilde{l}_I H^-}^L \Gamma_{\tilde{l}_I A^0}^R \Gamma_{A^0 H^+ W^-}^L \Gamma_{\tilde{c} b W^-}^L}{16\pi^2 M_{W^\pm}^2} C_{00}(m_l^2, M_{H^-}^2, m_{A^0}^2). \quad (21)$$

The Wilson coefficients $C_{VL}^{(H^0, h^0)}$ can be obtained from $C_{VL}^{A^0}$ by exchanging $A^0 \leftrightarrow (H^0, h^0)$. The corresponding couplings are given by

$$\Gamma_{\tilde{\chi}_j^- \nu_{l_I} \tilde{\tau}_i^*}^L = g(-Z_L^{iI*} Z_-^{j1*} + \frac{m_{l_I}}{\sqrt{2} M_{W^\pm} \cos \beta} Z_L^{i(I+3)*} Z_-^{j2}), \quad (22)$$

$$\Gamma_{\tilde{l}_I \tilde{\chi}_k^0 \tilde{\tau}_i}^R = \frac{g}{\sqrt{2}} (Z_L^{iI*} (\tan \theta_W Z_N^{k1*} + Z_N^{k2*}) - \frac{m_{l_I}}{M_{W^\pm} \cos \beta} Z_L^{i(I+3)*} Z_N^{j3*}), \quad (23)$$

$$\Gamma_{\tilde{\chi}_k^0 \nu_{l_I} \tilde{\nu}_i}^L = \frac{g}{\sqrt{2}} Z_\nu^{iI*} (\tan \theta_W Z_N^{k1} - Z_N^{k2}), \quad (24)$$

$$\Gamma_{\tilde{l}_I \tilde{\chi}_j^- \tilde{\nu}_i}^R = -g Z_+^{j1*} Z_\nu^{iI}, \quad \Gamma_{\tilde{c} b W^+}^L = -\frac{g}{\sqrt{2}} V_{cb}, \quad (25)$$

$$\Gamma_{\tilde{\chi}_j^+ \tilde{\chi}_k^0 W^-}^L = -g(Z_-^{j1} Z_N^{k2*} + \frac{1}{\sqrt{2}} Z_-^{j2} Z_N^{k3*}), \quad (26)$$

$$\Gamma_{\tilde{\chi}_j^+ \tilde{\chi}_k^0 W^-}^R = -g(Z_+^{j1} Z_N^{k2*} - \frac{1}{\sqrt{2}} Z_+^{j2} Z_N^{k4*}), \quad (27)$$

$$\Gamma_{\tilde{\tau} \nu H^-}^L = \frac{gm_\tau}{\sqrt{2} M_{W^\pm} \cos \beta} Z_{H^-}^{21}, \quad \Gamma_{A^0 H^+ W^-} = \frac{g}{2}, \quad (28)$$

$$\Gamma_{\tilde{\tau} \tau A^0}^R = -\frac{1}{\sqrt{2}} \frac{gm_\tau}{\sqrt{2} M_{W^\pm} \cos \beta} Z_A^{21}, \quad (29)$$

$$\Gamma_{\tilde{\tau} \tau H^0}^R = \frac{1}{\sqrt{2}} \frac{gm_\tau}{\sqrt{2} M_{W^\pm} \cos \beta} Z_H^{21}, \quad (30)$$

$$\Gamma_{H^0 H^+ W^-} = \frac{g}{2} (Z_H^{22} Z_{H^-}^{22} - Z_H^{21} Z_{H^-}^{21}), \quad (31)$$

where Z_L , Z_ν , Z_\pm , Z_N and $Z_{(H,A,H^-)}$ are the diagonalising matrices for slepton, sneutrino, chargino, neutralino and Higgs masses, respectively. In addition, the loop functions are given by [24]

$$B_0(x, y) = \eta_\epsilon - 1 + \log \frac{x}{\tilde{\mu}^2} - \frac{y \log \frac{y}{x}}{x - y}, \quad (32)$$

$$C_0(x, y, z) = \frac{1}{y - z} \left(\frac{y \log \frac{y}{x}}{y - x} + \frac{z \log \frac{z}{x}}{x - z} \right), \quad (33)$$

$$C_{00}(x, y, z) = \frac{1}{4} \left(\eta_\epsilon - \log \frac{x}{\tilde{\mu}^2} \right) + \frac{3}{8} + \frac{1}{y - z} \left(\frac{y^2 \log \frac{y}{x}}{4(x - y)} - \frac{z^2 \log \frac{z}{x}}{4(x - z)} \right), \quad (34)$$

with $\eta_\epsilon = \frac{2}{d-4} + \log 4\pi\gamma_E$, which is subtracted in the $\overline{\text{DR}}$ scheme, and $\tilde{\mu}$ the renormalisation scale with the dimensions of mass. Here, a few comments are in order. (i) The loop function $C_0(m_{\tilde{\chi}_k^0}^2, m_{\tilde{\chi}_j^-}^2, m_{\tilde{\tau}_i}^2) \rightarrow 0$ if

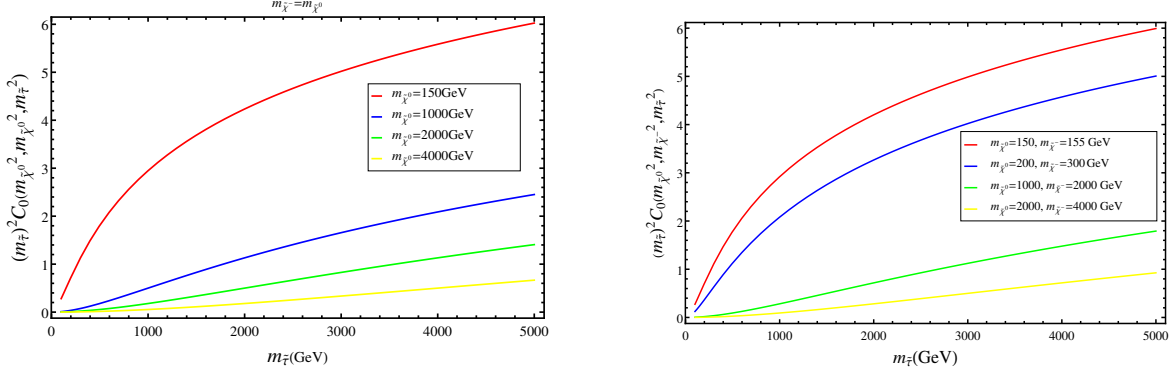


Figure 3: Behaviour of the last term in Eq. (19), $m_{\tilde{\tau}}^2 C_0(m_{\tilde{\chi}_0^0}^2, m_{\tilde{\chi}_-^0}^2, m_{\tilde{\tau}}^2)$, with $m_{\tilde{\tau}}$ for degenerate (left) and non-degenerate (right) chargino/neutralino masses.

$m_{\tilde{\chi}_k^0}, m_{\tilde{\chi}_j^-}$ and $m_{\tilde{\tau}_i} \rightarrow \infty$, as expected in the SUSY decoupling limit. (ii) If $m_{\tilde{\chi}_k^0}$ and $m_{\tilde{\chi}_j^-}$ are of order $\mathcal{O}(100)$ GeV and $m_{\tilde{\tau}_i}$ is very heavy, then $m_{\tilde{\tau}_i}^2 C_0(m_{\tilde{\chi}_k^0}^2, m_{\tilde{\chi}_j^-}^2, m_{\tilde{\tau}_i}^2)$ does not vanish, as this is not a decoupling limit since a light fermionic SUSY spectrum is assumed. Specifically, for $m_{\tilde{\chi}_k^0} \simeq m_{\tilde{\chi}_j^-}$, the loop function takes the form

$$C_0(m_{\tilde{\chi}_i^0}^2, m_{\tilde{\chi}_i^0}^2, m_{\tilde{\tau}_j}^2) = \frac{1}{(m_{\tilde{\chi}_i^0}^2 - m_{\tilde{\tau}_j}^2)^2} \left[m_{\tilde{\chi}_i^0}^2 - m_{\tilde{\tau}_j}^2 + m_{\tilde{\tau}_j}^2 \log \left(\frac{m_{\tilde{\tau}_j}^2}{m_{\tilde{\chi}_i^0}^2} \right) \right]. \quad (35)$$

(iii) From Eq. (19), one can see that, if $C_0(m_{\tilde{\chi}_i^0}^2, m_{\tilde{\chi}_i^0}^2, m_{\tilde{\tau}_j}^2) \neq 0$, then the last term, proportional to $m_{\tilde{\tau}_j}^2 C_0(m_{\tilde{\chi}_i^0}^2, m_{\tilde{\chi}_i^0}^2, m_{\tilde{\tau}_j}^2)$, gives the dominant effect to $C_{VL}^{\tilde{\tau}}$. (iv) The typical values of the couplings $\Gamma_{\tilde{\chi}_j^- \tilde{l}_i \tilde{\nu}_i}^R$, $\Gamma_{\nu_{l_i} \tilde{\chi}_k^0 \tilde{\nu}_i^*}^L$, $\Gamma_{\tilde{c} b W^-}^L$, $\Gamma_{\tilde{\chi}_j^+ \tilde{\chi}_k^0 W^-}^L$ and the loop function $C_0(m_{\tilde{\chi}_i^0}^2, m_{\tilde{\chi}_i^0}^2, m_{\tilde{\tau}_j}^2)$ at $m_{\tilde{\chi}_i^0} \sim \mathcal{O}(100)$ GeV and $m_{\tilde{\tau}_j} \sim \mathcal{O}(1)$ TeV imply that $C_{VL}^{\tilde{\tau}} \sim \frac{2 \times 10^{-3}}{16 \pi^2 M_{W^\pm}^2} m_{\tilde{\tau}_j}^2 C_0(m_{\tilde{\chi}_i^0}^2, m_{\tilde{\chi}_i^0}^2, m_{\tilde{\tau}_j}^2)$ is of order 10^{-8} GeV $^{-2}$. Therefore, $g_{VL} = C_{VL}^{\tilde{\tau}} / C^{\text{SM}}$, where $C^{\text{SM}} \sim 1.38 \times 10^{-6}$ GeV $^{-2}$, can be of order 0.01.

In Fig. 3 we show the behaviour of the last term in Eq. (19), $m_{\tilde{\tau}_i}^2 C_0(m_{\tilde{\chi}_k^0}^2, m_{\tilde{\chi}_j^-}^2, m_{\tilde{\tau}_i}^2)$ with several examples of degenerate (left panel) and non-degenerate (right panel) chargino/neutralino masses. As it can be seen from this figure, the largest corrections are obtained if chargino/neutralino masses are less than 200 GeV and the stau mass is larger than 1 TeV. It is further clear that, in the light gaugino mass regime, chargino/neutralino mass degeneracy is not a pre-condition for enhancing the aforementioned loop contribution, it so happens that there can be spectrum configurations in the scan when they are close in mass, as allowed by experimental constraints [25]. We stress again that, even if the stau is very heavy, we are not in the decoupling limit, where SUSY effects must diminish, since charginos/neutralinos are kept quite light.

Finally, the Wilson coefficients $C^{\text{SUSY}}(W \rightarrow l\nu)$ and $C^{\text{SUSY}}(\tau \rightarrow \nu_\tau l\nu_l)$ can be obtained from Eqs. (18) and (19) as follows

$$C^{\text{SUSY}}(\tau \rightarrow \nu_\tau l\nu_l) = \frac{\Gamma_{\tilde{\nu}_\tau \tau W^-}^L}{\Gamma_{\tilde{c} b W^-}^L} (C_{VL}^{\tilde{\tau}} + C_{VL}^{\tilde{\nu}}), \quad (36)$$

$$C^{\text{SUSY}}(W \rightarrow l\nu) = \frac{M_{W^\pm}^2}{\Gamma_{\tilde{c} b W^-}^L} (C_{VL}^{\tilde{\tau}} + C_{VL}^{\tilde{\nu}}), \quad (37)$$

where the loop functions are given by the following changes:

$$C_0(0, 0, 0, m_{\chi_k^0}^2, m_{\chi_j^-}^2, m_{\tilde{\nu}_i}^2) \rightarrow C_0(m_W^2, 0, 0, m_{\chi_k^0}^2, m_{\chi_j^-}^2, m_{\tilde{\nu}_i}^2), \quad (38)$$

$$C_{00}(0, 0, 0, m_{\chi_k^0}^2, m_{\chi_j^-}^2, m_{\tilde{\nu}_i}^2) \rightarrow C_{00}(m_W^2, 0, 0, m_{\chi_k^0}^2, m_{\chi_j^-}^2, m_{\tilde{\nu}_i}^2), \quad (39)$$

$$B_0(0, m_{\chi_k^0}^2, m_{\chi_j^-}^2) \rightarrow B_0(m_W^2, m_{\chi_k^0}^2, m_{\chi_j^-}^2), \quad (40)$$

where the loop functions of non-vanishing M_{W^\pm} can be found in [26, 27].

4 Experimental Constraints

Let us now discuss experimental limits coming from other processes. In this regard, one should consider a possible constraint due to the direct measurement of the W^\pm boson decay widths that leads to [28]

$$\Gamma(W \rightarrow \tau\nu)/\Gamma(W \rightarrow e\nu) = 1.043 \pm 0.024. \quad (41)$$

The SM prediction for this ratio is given by ~ 0.999267 , which is consistent with the measured value. Similarly, constraints can also be obtained from [28]

$$\Gamma(W \rightarrow \tau\nu)/\Gamma(W \rightarrow \mu\nu) = 1.07 \pm 0.026, \quad (42)$$

with which the SM is also consistent. The decay width of $W \rightarrow l\nu$ with SUSY contributions can be parametrised as

$$\Gamma(W \rightarrow l\nu) = \frac{G_F M_{W^\pm}^3}{6\sqrt{2}\pi} \left(1 - \frac{m_l^2}{M_{W^\pm}^2}\right)^2 \left(1 + \frac{1}{2} \frac{m_l^2}{M_{W^\pm}^2}\right) |1 + g'_{VL}|^2, \quad (43)$$

where $g'_{VL} = C^{\text{SUSY}}(W \rightarrow l\nu)/C^{\text{SM}}(W \rightarrow l\nu)$ and $C^{\text{SM}}(W \rightarrow l\nu) = g/\sqrt{2}$. Another important experimental measurement connected with lepton universality in τ decay that should be considered here is of $\tau \rightarrow \nu_\tau l \nu_l$ with $l = e, \mu$, which is given by the relation² [31]

$$\left(\frac{g_\mu}{g_e}\right)_\tau = \frac{BR(\tau \rightarrow \mu\nu_\tau\nu_\mu) f(m_e^2/m_\tau^2)}{BR(\tau \rightarrow e\nu_\tau\nu_e) f(m_\mu^2/m_\tau^2)}. \quad (44)$$

In the SM, the universal gauge interaction implies that

$$\frac{\Gamma(\tau \rightarrow \mu\nu_\tau\nu_\mu)}{\Gamma(\tau \rightarrow e\nu_\tau\nu_e)} = \frac{f(m_\mu^2/m_\tau^2)}{f(m_e^2/m_\tau^2)} = 0.9726, \quad (45)$$

where $f(x) = 1 - 8x + 8x^3 - x^4 - 12x^2 \log(x)$. The current experimental result for this ratio is 0.979 ± 0.004 [28], which gives $\left(\frac{g_\mu}{g_e}\right)_\tau = 1.0032 \pm 0.002$. With SUSY contributions, Eq. (45) can be written as

$$\frac{\Gamma(\tau \rightarrow \mu\nu_\tau\nu_\mu)}{\Gamma(\tau \rightarrow e\nu_\tau\nu_e)} = 0.9726 \frac{|1 + g_{VL}^\mu|^2}{|1 + g_{VL}^e|^2}, \quad (46)$$

where $g_{VL}^l = C^{\text{SUSY}}(\tau \rightarrow \nu_\tau l \nu_l)/C^{\text{SM}}(\tau \rightarrow \nu_\tau l \nu_l)$ with $C^{\text{SM}}(\tau \rightarrow \nu_\tau l \nu_l) = 2\sqrt{2}G_F$. (As we will show, this imposes stringent constraints on SUSY contributions to g_{VL}^l). Furthermore, SUSY loop effects induce a correction to the Fermi coupling via a potential breaking of $\mu - e$ universality. In fact, using Eqs. (44) and (46), for $g_{VL}^l \ll 1$ one can find

$$\left(\frac{g_\mu}{g_e}\right)_\tau = \frac{|1 + g_{VL}^\mu|}{|1 + g_{VL}^e|} = |1 + \Delta g_{VL}^{\mu,e}|, \quad (47)$$

²In the presence of NP, the deviations from $\tau - \mu - e$ universality can be studied via the ratios of the branching fractions $BR(\tau \rightarrow \nu_\tau e \nu_e)/BR(\mu \rightarrow \nu_\mu e \nu_e)$, $BR(\tau \rightarrow \nu_\tau \mu \nu_\mu)/BR(\mu \rightarrow \nu_\mu e \nu_e)$, $BR(\tau \rightarrow \nu_\tau \mu \nu_\mu)/BR(\tau \rightarrow \nu_\tau e \nu_e)$, which lead to appropriate ratios $G_{\tau,e}/G_{\mu,e}$, $G_{\tau,\mu}/G_{\mu,e}$ and $G_{\tau,\mu}/G_{\tau,e}$, respectively. Here we use a different convention from those in Refs. [29, 30], *i.e.*, we take the ratio $(g_\mu/g_e)_\tau$ rather than $(G_{\tau,\mu}/G_{\tau,e})$.

where $\Delta g_{VL}^{\mu,e} = g_{VL}^{\mu} - g_{VL}^e$, so that the above experimental constraints impose that $0.0012 \leq \Delta g_{VL}^{\mu,e} \leq 0.0052$. In our work, we will enforce $g_{\mu} = g_e = g$, which satisfies Eq. (47).

Moreover, there are other constraints that could be considered here, coming from Lepton Flavour Violating (LFV) processes such as $\text{BR}(\tau^- \rightarrow \mu^- \gamma) < 4.5 \times 10^{-8}$ and $\text{BR}(\tau^- \rightarrow e^- \gamma) < 1.2 \times 10^{-7}$ [32] as well as $\text{BR}(H \rightarrow e\tau) < 1.04\%$, $\text{BR}(H \rightarrow \mu\tau) < 1.43$ and $\text{BR}(Z \rightarrow \mu\tau) < 1.69 \times 10^{-5}$ [33]. However, we will focus on the strongest one, which is indeed from the decay $\tau \rightarrow l\nu_{\tau}\nu_l$, as shown above, essentially because it carries the same one-loop corrections of the vertex $W^{\pm}l\nu_l$ within the process $b \rightarrow cl\nu_l$. Furthermore, the lifetime of the B_c meson may also impose important constraints on the scalar contributions, g_{SL} and g_{SR} . However, this observable is less sensitive to the vector contribution, g_{VL} , which is playing an important role in enhancing $R(D)$ and $R(D^*)$ in our analysis. This has been discussed in detail in Ref. [35]. In summary, in our scans, only points respecting all the above limits are retained. In particular, compliance with Eqs. (41)–(42) ensures that our parameter space automatically satisfies also constraints from the ratio $\Gamma(\tau \rightarrow e\nu\nu)/\Gamma(\mu \rightarrow e\nu\nu)$. Indeed, the SUSY contribution to $\mu \rightarrow e\nu\nu$ leads to $\text{BR}(\mu \rightarrow e\nu\nu) \approx 100\%$, which is consistent with the experimental result given in Ref. [28].

Furthermore, the oblique Electro-Weak (EW) parameters S , T and U [34] are useful to constraint NP that enters in self-energy corrections to a gauge boson propagator, denoted by Π_{ij} , which represents the transition ij ($i, j = W, Z, \gamma$), as we have [28]

$$\hat{\alpha}(M_Z)T = \frac{\Pi_{WW}^{\text{NP}}(0)}{M_W^2} - \frac{\Pi_{ZZ}^{\text{NP}}(0)}{m_Z^2}, \quad (48)$$

where $\hat{\alpha}(M_Z)$ is the renormalised Electro-Magnetic (EM) coupling constant at the M_Z scale. Here, we are interested in the T parameter. In this respect, a related quantity known as the ρ parameter is defined as [28]

$$\rho - 1 = \frac{1}{1 - \hat{\alpha}(M_Z)T} \simeq \hat{\alpha}(M_Z)T. \quad (49)$$

In this work we take $\Delta\rho^{\text{exp}} = \rho - 1 = 0.0006 \pm 0.0009$, which is extracted from the data on the T parameter (0.08 ± 0.12) [28]. While in the SM $\rho \equiv \rho_0 = M_{W^{\pm}}^2/M_Z^2 \cos^2 \theta_W = 1$ at tree level, in our scan we obtain $\Delta\rho^{\text{SUSY}} \in [0.0001, 0.0006]$.

5 Numerical Analysis

We now perform the numerical evaluations in the light of the results in Sects. 2 and 3 in presence of experimental constraints. Since our focus is on the penguin contributions, let us look at the relevant loop functions entering the numerics. Let us begin with those of $W \rightarrow l\nu$, from the formulae given in Eq. (38) one can notice that the loop functions of the decay $W \rightarrow l\nu$ are approximately equal to those associated with $b \rightarrow cl\nu$: this is made evident in Tab. 1, for the case of the MSSM benchmark of Tab. 2, which is one yielding sizable corrections to both $R(D)$ and $R(D^*)$.

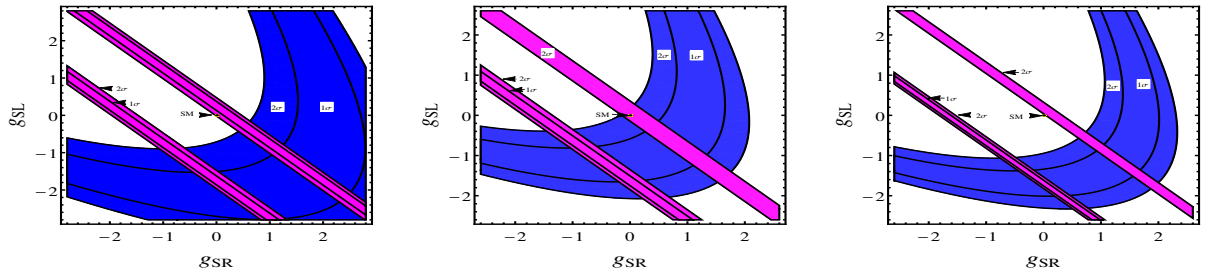


Figure 4: The allowed regions in the (g_{SL}, g_{SR}) plane by the 1σ and 2σ experimental results on $R(D)$ (magenta) and $R(D^*)$ (blue) of BaBar (left), Belle (middle) and combined average (right). SM and complete SUSY predictions (tree, penguin and box contributions, where tree-level effect is the dominant for the scalar interactions) are also included and they coincide with the black point.

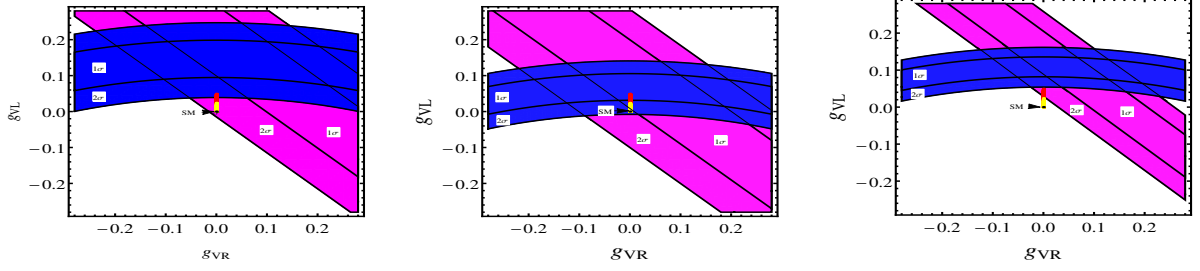


Figure 5: The allowed regions in the (g_{VL}, g_{VR}) plane by the 1σ and 2σ experimental results on $R(D)$ (magenta) and $R(D^*)$ (blue) of BaBar (left), Belle (middle) and combined average (right). SM (black point) and complete SUSY (red points) predictions (penguin and box contributions, where the penguin is the dominant one) are also included.

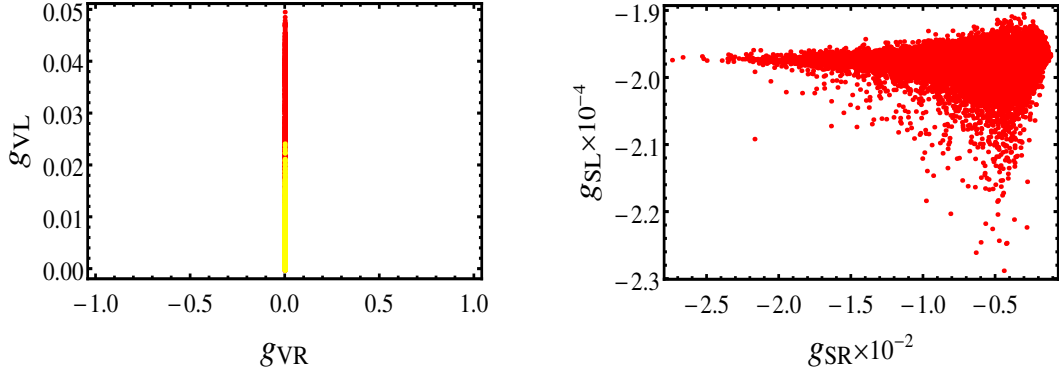


Figure 6: (Left) The correlation between the SUSY corrected values of g_{VL} and g_{VR} is displayed in the right panel, where yellow points represent the configurations that yield $\Gamma(\tau \rightarrow \mu\nu_\tau\nu_\mu)/\Gamma(\tau \rightarrow e\nu_\tau\nu_e)$ within experimental limits while the red ones are the complete sample. (Right) The correlation between the SUSY corrected values of g_{SL} and g_{SR} is displayed in the right panel.

In essence, the one-loop SUSY effects onto the W^\pm widths are scaled by the W^\pm squared mass while in $R(D)$ and $R(D^*)$ only by the meson squared masses. These suppressions are crucial for satisfying the experimental constraints on the ratio of the W^\pm decay widths so that the results of $R(D)$ and $R(D^*)$ can be accommodated in unexcluded regions of the MSSM parameter space.

As mentioned, the enhancement of C_{VL}^{τ} occurs mostly when the chargino and neutralino masses are light and similar, in addition to large $\tan\beta$ and stau mass. Therefore, in our scan, we focus on benchmark points where the gaugino soft masses are given by $M_1, M_2 \in [110, 500]$ GeV and $M_3 = 2$ TeV. Also, we choose the μ parameter $\in [100, 500]$ GeV, $m_{A^0}^2 \in [0, 25 \times 10^4]$ GeV², the A terms $\in [-2000, -100]$ GeV, $M_{\tilde{Q}}, M_{\tilde{U}}$ and $M_{\tilde{D}}$ are fixed in the TeV range while the slepton soft mass terms $m_{\tilde{L}}$ and $m_{\tilde{E}}$ $\in [100, 5000]$ GeV. Finally, we take $\tan\beta \in [5, 70]$. (As mentioned, the aforementioned Tab. 2 shows an example yielding large corrections to our two observables extracted from such a scan.)

In Figs. 4 and 5 we display the regions in the (g_{SL}, g_{SR}) and (g_{VL}, g_{VR}) planes, respectively, that can accommodate the BaBar, Belle and combined average results on $R(D)$ and $R(D^*)$ within a 1σ and 2σ CL. We also compare these ranges with the MSSM expectations at the one-loop level. It is clear that the contributions that induce vector operators, like the aforementioned triangle diagrams, lead to $R(D)$ and $R(D^*)$ close to or potentially within the experimental regions. We can also conclude that g_{VL} must be non-vanishing and of order 0.1 while g_{VR} can be in the range $[-0.1, 0.1]$. This conclusion is explicitly confirmed in Fig. 6, where the correlation between the SUSY contribution to g_{VL} and g_{VR} is presented. As expected, $g_{VR} \sim 0$ in the MSSM, which has no right-handed vector contribution, while g_{VL} can be of order few percents, which can account for the Belle results within the 1σ

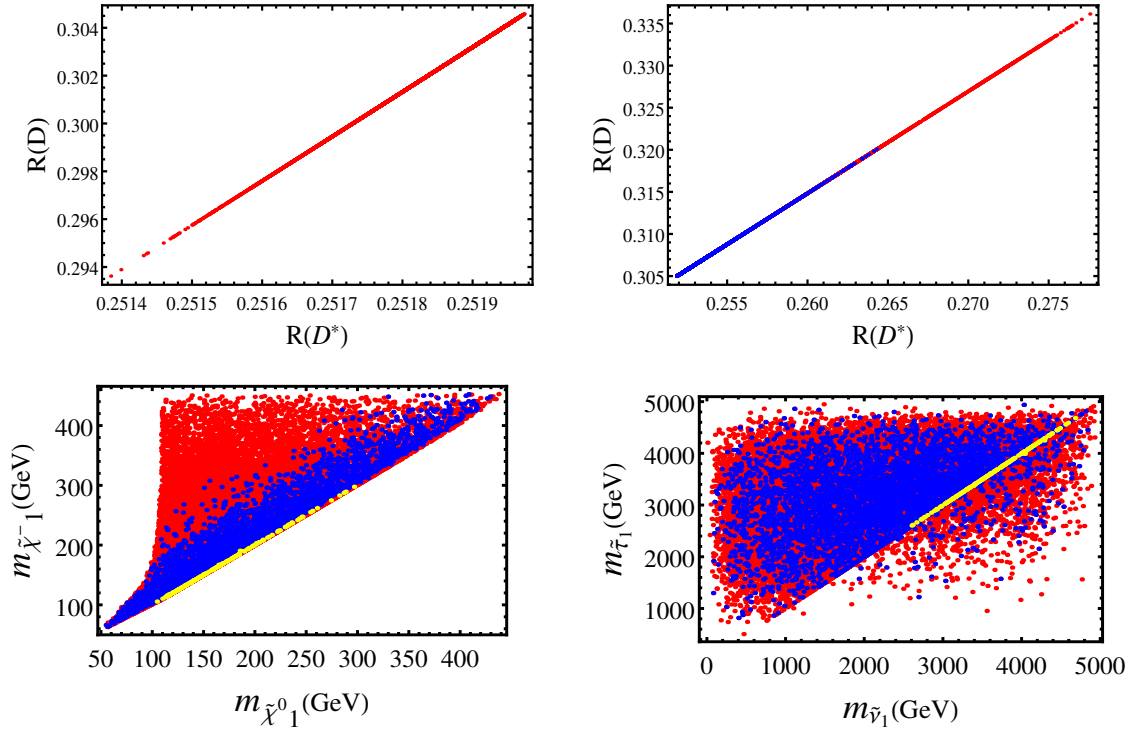


Figure 7: The correlation between $R(D)$ and $R(D^*)$ at tree level (top-left) and after the one-loop SUSY contributions through the lepton penguins (top-right) where the blue points show the constrained ones by $\Gamma(\tau \rightarrow \mu\nu_\tau\nu_\mu)/\Gamma(\tau \rightarrow e\nu_\tau\nu_e)$. The correlation between sneutrino and stau masses is on the bottom-left (same colour scheme as in the top-right frame with the additional yellow points representing the region with $R(D) > 0.33$). (Bottom-right) This represents the correlation between chargino and neutralino masses where the colours have the same meaning as in the bottom-left panel.

limit and on the borderline with the 2σ band of BaBar and average results. Herein, SUSY contributions to g_{SL} and g_{SR} , which are negligibly small, $\sim 10^{-4}$, are also displayed.

In the top-left (top-right) panel of Fig. 7 we present the correlation between $R(D)$ and $R(D^*)$ at tree-level (at one-loop due to the SUSY contributions to the lepton penguins alone). As can be seen from this plot, in presence of MSSM one-loop corrections, $R(D)$ can reach 0.335 while $R(D^*)$ extends to 0.277, which are results rather consistent with the Belle measurements and not that far from the BaBar ones. This correlation can be understood from the fact that SUSY one-loop corrections give a significant contribution to g_{VL} only (of order 6%) and, hence, according to Eqs. (15)–(16), both $R(D)$ and $R(D^*)$ are affected by the same correction factor $\propto (1 + g_{VL})^2$ through a common Wilson coefficient. It is also worth noting that the enhancements of $R(D)$ and $R(D^*)$ require a very peculiar region of parameter space of the MSSM, especially in terms of $m_{\tilde{\chi}_1^-}$ and $\tan\beta$, wherein, however, all experimental and theoretical constraints sensitive to the latter two quantities are taken into account and included in our scan and numerical analysis. To our knowledge, these enhancements in both $R(D)$ and $R(D^*)$ have never been accounted for before in any NP scenario. The dependence of $R(D)$ and $R(D^*)$ on $\tan\beta$ is displayed in Fig. 8. As can be seen from these plots, a larger value of $\tan\beta$ is preferred by larger values of $R(D)$ and $R(D^*)$. This can be understood from Eqs. (22) and (31) that emphasise the increase of the neutralino and chargino couplings with the τ lepton at very large $\tan\beta$.

It is also very relevant to extract the typical mass spectra which are responsible for the MSSM configurations yielding $R(D)$ and $R(D^*)$ values (potentially) consistent with experimental measurements, as these might be accessible during Run 3 at the LHC. As an indication, this is done in Fig. 7 (bottom-left panel) for the case of

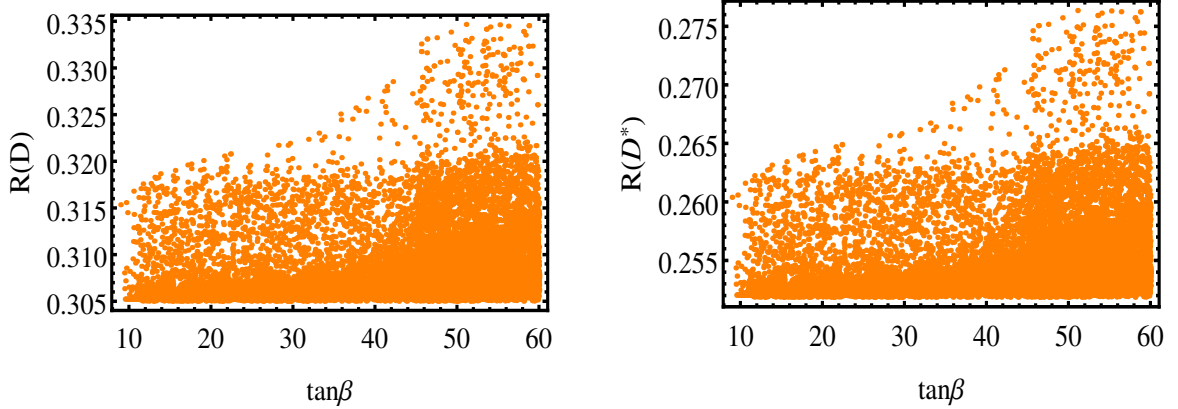


Figure 8: $R(D)$ and $R(D^*)$ as functions of $\tan\beta$. The scan over the parameter space is performed as in the previous plots.

the lightest stau and sneutrino. The plot shows a predilection of the highest $R(D)$ and $R(D^*)$ points for MSSM parameter configurations with $m_{\tilde{\tau}_1} > m_{\tilde{\nu}_1}$ while the absolute mass scale can cover the entire interval from 200 GeV to 5 TeV. However, the points with $R(D) > 0.33$ require a rather large $\tilde{\tau}_1$ mass (say above 2.5 TeV) irrespectively of the $\tilde{\nu}_1$ one as well as large $\tan\beta$. This signals that there occurs an interplay between mass suppressions in the loops and enhancements in the couplings.

6 Conclusions

In summary, we have proven that the MSSM has the potential to alleviate the anomaly presented by recent data produced by especially Belle and (somewhat less so) BaBar, which revealed a rather significant excess above and beyond the best SM predictions available in the observed $\text{BR}(\bar{B} \rightarrow D\tau\bar{\nu}_\tau)$ and $\text{BR}(\bar{B} \rightarrow D^*\tau\bar{\nu}_\tau)$ relative to the light lepton cases. Most remarkably, within the MSSM, the excesses can be explained *simultaneously*, needless to say, over the same regions of parameter space. Further, the latter do not correspond to any particularly fine-tuned dynamics (possibly apart from light neutralino/chargino masses, plus a preference for heavy $\tilde{\tau}_1$ and $\tilde{\nu}_1$, recall Fig. 7) and a more than acceptable agreement with the Belle (especially) and BaBar (to a lesser extent) data can be reached via MSSM spectra easily compatible with current experimental constraints from a variety of sources (flavour physics, Higgs boson measurements, SUSY searches). Such a conclusion is obtained after the *first complete* tree-level plus (penguin dominated) one-loop calculation of all MSSM topologies entering the partonic $b \rightarrow c\tau\nu_\tau$ decay process matched with standard computational elements enabling the transition from the partonic to hadronic level. If forthcoming data will confirm the anomalous BaBar and Belle results, e.g., from the now running LHCb experiment at the LHC, our findings are rather interesting since a variety of other (typically non-SUSY) models have been tried and tested as a possible explanation of the $\bar{B} \rightarrow D\tau\bar{\nu}_\tau$ and $\bar{B} \rightarrow D^*\tau\bar{\nu}_\tau$ anomalies and failed. On the one hand, our results might then be taken as a circumstantial evidence of SUSY. On the other hand, they might pave the way to its direct discovery as they point to spectra in the sparticle sector of the MSSM that can be accessed at Run 3.

Acknowledgments

SK is supported from the STDF project 13858. DB is supported by the Algerian Ministry of Higher Education and Scientific Research under the PNE Fellowship and CNEPRU Project No. B00L02UN180120140040. SM is supported through the NExT Institute. All authors acknowledge support from the grant H2020-MSCA-RISE-2014 n. 645722 (NonMinimalHiggs) and thank A. Vicente and F. Staub for help.

Loop function	$b \rightarrow c\tau\nu_\tau$	$W \rightarrow \tau\nu_\tau$
C_{00}	-1.2880	-1.2879
C_0	$2.910 \times 10^{-7} \text{ GeV}^{-2}$	$2.931 \times 10^{-7} \text{ GeV}^{-2}$
B_0	0.0281	0.0715

Table 1: Loop functions values which correspond to the benchmark given in Tab. 2, where the renormalisation scale, $\tilde{\mu}$, has been fixed at 1 GeV.

Parameter	Value
$\tan \beta$	55.22
μ	432.05 GeV
$M_{A^0}^2$ (tree)	$2.5 \times 10^5 \text{ GeV}$
M_1, M_2, M_3	326.59, 169.40, 2000 GeV
$M_{\tilde{U}}, M_{\tilde{D}}, M_{\tilde{Q}}$	1 TeV (all)
$M_{\tilde{E}_1}, M_{\tilde{E}_2}, M_{\tilde{E}_3}$	1693.70, 4926.31, 1033.35 GeV
$M_{\tilde{L}_1}, M_{\tilde{L}_2}, M_{\tilde{L}_3}$	4877.02, 4910.96, 4446.64 GeV
A_t, A_b, A_τ	-1806.83, -1887.99, 0 GeV
$m_{\tilde{\chi}_1^0}, m_{\tilde{\chi}_1^-}$	173.07, 173.52 GeV
$m_{\tilde{\nu}_1}, m_{\tilde{\tau}_1}$	4466.25, 4467.40 GeV
$M_{h^0}, M_{H^0}, M_{A^0}, M_{H^\pm}$	125.13, 441.72, 441.87, 405.60 GeV
$\Gamma_{\tilde{\chi}_1^- \nu_\tau \tilde{\tau}_1^*}^L$	0.629
$\Gamma_{\tilde{\chi}_1^- \bar{\tau} \tilde{\nu}_1}^R$	-0.656
$\Gamma_{\tilde{\tau} \tilde{\chi}_1^0 \tilde{\tau}_1}^R$	-0.447
$\Gamma_{\nu_\tau \tilde{\chi}_1^0 \tilde{\nu}_1^*}^L$	-0.460
$\Gamma_{\tilde{\chi}_1^+ \chi_1^0 W^-}^R$	-0.642
$\Gamma_{\tilde{\chi}_1^+ \chi_1^0 W^-}^L$	-0.642
$\Gamma_{\tilde{e} b W^-}^L$	-0.019
$\tilde{g}_{VL}^{\tilde{\tau}}(b \rightarrow c\tau\bar{\nu}_\tau)$	0.021
$\tilde{g}_{VL}^{\tilde{\nu}}(b \rightarrow c\tau\bar{\nu}_\tau)$	0.022
$\tilde{g}_{VL}^{H^0, A^0, H^\pm}(b \rightarrow c\tau\bar{\nu}_\tau)$	0.0042
$g_{VL}(b \rightarrow c\tau\bar{\nu}_\tau) = \tilde{g}_{VL}^{\tilde{\tau}} + \tilde{g}_{VL}^{\tilde{\nu}} + \tilde{g}_{VL}^{H^0, A^0, H^\pm}$	0.047
$g_{VL}(b \rightarrow ce\bar{\nu}_e)$	0
$R(D)$	0.335
$R(D^*)$	0.276

Table 2: Illustrative benchmark point yielding large $R(D)$ and $R(D^*)$ values.

References

- [1] Belle Collaboration, Phys. Rev. D **92**, no. 7, 072014 (2015).
- [2] Y. Sato *et al.* [Belle Collaboration], Phys. Rev. D **94**, no. 7, 072007 (2016).
- [3] Belle Collaboration, arXiv:1603.06711 [hep-ex].
- [4] S. Hirose *et al.* [Belle Collaboration], Phys. Rev. Lett. **118**, no. 21, 211801 (2017).
- [5] BaBar Collaboration, Phys. Rev. D **88**, 072012 (2013).
- [6] LHCb Collaboration, Phys. Rev. Lett. **115**, no. 11, 111803 (2015).
- [7] Y. Amhis *et al.*, Eur. Phys. J. C **77**, no. 12, 895 (2017).
- [8] M. Tanaka and R. Watanabe, Phys. Rev. D **87**, 034028 (2013).
- [9] Y. Sakaki, M. Tanaka, A. Tayduganov and R. Watanabe, Phys. Rev. D **88**, 094012 (2013).
- [10] Y. Sakaki, M. Tanaka, A. Tayduganov and R. Watanabe, Phys. Rev. D **91**, no. 11, 114028 (2015).
- [11] S. Fajfer, J. F. Kamenik and I. Nisandzic, Phys. Rev. D **85**, 094025 (2012).
- [12] A. Crivellin, C. Greub and A. Kokulu, Phys. Rev. D **86**, 054014 (2012).
- [13] A. Crivellin, A. Kokulu and C. Greub, Phys. Rev. D **87**, no. 9, 094031 (2013).
- [14] A. Celis, M. Jung, X. Q. Li and A. Pich, JHEP **1301**, 054 (2013).
- [15] A. Celis, M. Jung, X. Q. Li and A. Pich, Phys. Lett. B **771**, 168 (2017).
- [16] S. Bhattacharya, S. Nandi and S. K. Patra, Phys. Rev. D **93**, 034011 (2016).
- [17] K. Hagiwara, A. D. Martin and M. F. Wade, Nucl. Phys. B **327**, 569 (1989).
- [18] K. Hagiwara, A. D. Martin and M. F. Wade, Phys. Lett. B **228**, 144 (1989).
- [19] A. Datta, M. Duraissamy and D. Ghosh, Phys. Rev. D **86**, 034027 (2012).
- [20] M. Duraissamy and A. Datta, JHEP **1309**, 059 (2013).
- [21] W. Porod, F. Staub and A. Vicente, Eur. Phys. J. C **74**, 2992 (2014).
- [22] F. Staub, Comput. Phys. Commun. **185**, 1773 (2014).
- [23] W. Porod and F. Staub, Comput. Phys. Commun. **183**, 2458 (2012).
- [24] A. J. Buras, P. H. Chankowski, J. Rosiek and L. Slawianowska, Nucl. Phys. B **659**, 3 (2003).
- [25] B. Fuks, M. Klasen, S. Schmiemann and M. Sunder, Eur. Phys. J. C **78** no.3, 209 (2018).
- [26] J. C. Romão, <http://porthos.tecnico.ulisboa.pt/OneLoop/one-loop.pdf>.
- [27] W. F. L. Hollik, Fortsch. Phys. **38**, 165 (1990).
- [28] C. Patrignani, Chin. Phys. C **40**, no. 10, 100001 (2016).
- [29] P. H. Chankowski, R. Hempfling and S. Pokorski, Phys. Lett. B **333**, 403 (1994).
- [30] A. Masiero, P. Paradisi and R. Petronzio, JHEP **0811**, 042 (2008).

- [31] BaBar Collaboration, Phys. Rev. Lett. **105**, 051602 (2010).
- [32] BaBar Collaboration, Phys. Rev. Lett. **104**, 021802 (2010).
- [33] G. Aad *et al.* [ATLAS Collaboration], Eur. Phys. J. C **77**, no. 2, 70 (2017).
- [34] M. E. Peskin and T. Takeuchi, Phys. Rev. Lett. **65**, 964 (1990).
- [35] R. Alonso, B. Grinstein and J. Martin Camalich, Phys. Rev. Lett. **118**, no. 8, 081802 (2017).